Activation of Na^+-permeant Cation Channel by Stretch and Cyclic AMP-dependent Phosphorylation in Renal Epithelial A6 Cells

Yoshinori Marunaka,*§ Yutaka Shintani,*§ Gregory P. Downey,‡|| and Naomi Niisato*§

From the *Laboratory for Cellular and Molecular Physiology, Division of Respiratory Research, Hospital for Sick Children Research Institute, ‡Division of Respirology, Department of Medicine, The Toronto Hospital, §Department of Paediatrics, and ||Department of Medicine, Faculty of Medicine, University of Toronto, Toronto, Ontario, Canada M5G 1X8

ABSTRACT It is currently believed that a nonselective cation (NSC) channel, which responds to arginine vasotocin (an antidiuretic hormone) and stretch, regulates Na^+ absorption in the distal nephron. However, the mechanisms of regulation of this channel remain incompletely characterized. To study the mechanisms of regulation of this channel, we used renal epithelial cells (A6) cultured on permeable supports. The apical membrane of confluent monolayers of A6 cells expressed a 29-pS channel, which was activated by stretch or by 3-isobutyl-1-methylxanthine (IBMX), an inhibitor of phosphodiesterase. This channel had an identical selectivity for Na^+, K^+, Li^+, and Cs^+, but little selectivity for Ca^{2+} ($P_{Ca}/P_{Na} < 0.005$) or Cl^- ($P_{Cl}/P_{Na} < 0.01$), identifying it as an NSC channel. Stretch had no additional effects on the open probability (P_o) of the IBMX-activated channel. This channel had one open ("O") and two closed (short "C_S" and long "C_L") states under basal, stretch-, or IBMX-stimulated conditions. Both stretch and IBMX increased the P_o of the channel without any detectable changes in the mean open or closed times. These observations led us to the conclusion that a kinetic model "$C_L \leftrightarrow C_S \leftrightarrow O$" was the most suitable among three possible linear models. According to this model, IBMX or stretch would decrease the leaving rate of the channel for C_L from C_S, resulting in an increase in P_o. Cytochalasin D pretreatment abolished the response to stretch or IBMX without altering the basal activity. H89 (an inhibitor of cAMP-dependent protein kinase) completely abolished the response to both stretch and IBMX, but, unlike cytochalasin D, also diminished the basal activity. We conclude that: (*a*) the functional properties of the cAMP-activated NSC channel are similar to those of the stretch-activated one, (*b*) the actin cytoskeleton plays a crucial role in the activation of the NSC channel induced by stretch and cAMP, and (*c*) the basal activity of the NSC channel is maintained by PKA-dependent phosphorylation but is not dependent on actin microfilaments.

KEY WORDS: nonselective cation channel • single channel • cytochalasin D • cyclic AMP • actin filament

INTRODUCTION

Antidiuretic hormone (ADH)[1] increases the water permeability of the apical membrane of distal nephron cells leading to a net increase in water absorption. Furthermore, ADH increases Na^+ transport in distal nephron cells (Garty and Benos, 1988; Smith and Benos, 1991; Palmer, 1992). Investigations using single channel recording (Marunaka and Eaton, 1991) have demonstrated that ADH also increases the number of 4-pS amiloride-sensitive, highly Na^+-selective channels. These channels are thought to play an important role in Na^+ reabsorption as the entry pathway of Na^+ across the apical membrane from the lumen to the intracellular space in aldosterone-treated A6 cells, an amphibian kidney cell line commonly used as a model of distal nephron cells (Perkins and Handler, 1981; Benos et al., 1986; Sariban-Sohraby et al., 1988; Marunaka and Eaton, 1990*a*, 1990*b*, 1991; Chalfant et al., 1993; Marunaka, 1993; Marunaka and Tohda, 1993). On the other hand, a gadolinium-sensitive stretch-activated nonselective cation (NSC) channel with a single channel conductance of 28 pS has been frequently observed in the apical membrane of A6 cells untreated with aldosterone, and arginine vasotocin (AVT; an ADH) activated this NSC channel (Marunaka et al., 1994). Further, in aldosterone-untreated A6 cells, an apical membrane gadolinium-sensitive channel has been suggested to contribute to Na^+ absorption (Marunaka, 1996*a*; Niisato and Marunaka, 1997*c*). Importantly, this latter channel retains full activity in the presence of 10 μM amiloride, which completely blocks the 4-pS amiloride-sensitive, highly Na^+-selective channel (Palmer, 1992). Taken together, these observations suggest that this 28-pS NSC channel plays a role in Na^+ absorption in the aldosterone-untreated distal nephron. Despite the potential importance of this channel, the mechanisms of its regulation, and, in particular, the relationship between

Address correspondence to Dr. Yoshinori Marunaka, Division of Respiratory Research, Hospital for Sick Children Research Institute, 555 University Avenue, Toronto, Ontario, Canada M5G 1X8. Fax: 416-813-5771; E-mail: marunaka@sickkids.on.ca

[1]*Abbreviations used in this paper:* ADH, antidiuretic hormone; AVT, arginine vasotocin; CD, cytochalasin D; I-V, current–voltage; IBMX, 3-isobutyl-1-methylxanthine; NSC, nonselective cation.

AVT- and stretch-induced activation of this NSC channel, remain unclear.

In an initial attempt to examine this issue, we studied the effect of stretch on the AVT-activated channel. However, because AVT-induced activation of the NSC channel is only transient (Marunaka et al., 1994), we were unable to clarify the relationship between the AVT and stretch action. Accordingly, we needed another means to stably activate the NSC channel in place of AVT. In this study, we report that 3-isobutyl-1-methylxanthine (IBMX, an inhibitor of phosphodiesterase), which increased cAMP (a second messenger of AVT), stably activated the NSC channel and that stretch had no effects on the IBMX-activated channel. Additionally, the single channel gating properties of the stretch-activated NSC channel were identical to those of the IBMX-activated one.

MATERIALS AND METHODS

Solutions

The bathing and pipette solutions used for single-channel recording in cell-attached patches contained (mM): 120 NaCl, 3.5 KCl, 1 $CaCl_2$, 1 $MgCl_2$, and 10 HEPES, pH 7.4 (standard solution). When the ion selectivity was determined in inside-out patches, the pipette solution contained (mM): 120 NaCl, 1 $CaCl_2$, 1 $MgCl_2$, and 10 HEPES, pH 7.4. The bathing (cytosolic) solution contained (mM): 120 KCl, 120 LiCl, 120 CsCl, 120 NMDG-Cl or 120 K-gluconate, instead of 120 NaCl with 1 $CaCl_2$, 1 $MgCl_2$, and 10 HEPES, pH 7.4. To study the Ca^{2+} permeability, 60 mM $CaCl_2$ with 1 mM $MgCl_2$ and 10 mM HEPES, pH 7.4, was used in the bathing solution.

Cell Line and Culture Methods

A6 cells were purchased from American Type Culture Collection (Rockville, MD) in the 68th plating. All experiments were carried out on the 71st–83rd platings; there were no discernible differences between cells from different platings. Cells were maintained in plastic tissue culture flasks (Corning Glass Works, Corning, NY) at 26°C in a humidified incubator with 4% CO_2 in air. The culture medium was an NCTC 109 medium (Gibco Laboratories, Grand Island, NY) modified for amphibian cells with 100 mM NaCl, 20 mM $NaHCO_3$, pH 7.4, containing 10% fetal bovine serum (Gibco Laboratories), 100 μg/ml streptomycin, and 100 U/ml penicillin (Irvine Scientific, Santa Ana, CA) (Doi and Marunaka, 1995; Nakahari and Marunaka, 1995, 1996). No supplemental aldosterone was added to the cell culture media.

Patch Recording

Standard patch-clamp techniques were used as previously described (Marunaka et al., 1992; Marunaka, 1996*b*). Patch pipettes were made from LG 16 glass (Dagan Corp., Minneapolis, MN). Patch pipettes were fire polished to produce tip diameters of ~0.5 μm. Single-channel currents were obtained at 22–23°C with an Axopatch 1D patch-clamp amplifier (Axon Instruments, Foster City, CA). An Ag-AgCl reference electrode was connected to a bathing solution via a 3% agar bridge containing 3 M KCl. Current signals were recorded on a digital video recorder (HF860D; Sony Corp., Tokyo, Japan) with pulse code modulation (1-DR-390; Neuro Data Instruments Corp., New York), and then digitized and analyzed by an IBM PC compatible computer with a continuous data-acquisition program. A 500-Hz low-pass filter using a software Gaussian filter was used to present the actual traces. To analyze the channel kinetics, a 2,000-Hz low pass Gaussian filter was used. When cells were used for patch-clamp experiments, cells from the flasks were subcultured on a permeable support filter (Nunc Tissue Culture Inserts; Nunc, Roskilde, Denmark). Cells plated on permeable supports (Nunc filter) formed polarized monolayers with their apical surfaces upward. The patch pipette was applied from the luminal side, and a gigaohm seal (>100 gigaohm) was made on the apical membrane of cells.

Open Probability (P_o) of a Single Channel

Channel activity is expressed as open probability (P_o):

$$P_O = \frac{1}{N}\sum_{i=1}^{N} (i \cdot P_i), \quad (1)$$

where n is the number of channels, P_o is the open probability of an individual channel, i is the number of channels being simultaneously open; P_i is the probability of only i channels being simultaneously open. As previously reported (Marunaka et al., 1994), the NSC channel studied in the present report was activated by stretch or depolarization of the membrane. By applying stretch or depolarization, which increased P_o, we could observe the current level of all the channels in the patch membrane that were simultaneously open. Further, without the application of stretch, the NSC channel demonstrated very little activity (low P_o). This led us to observe the current level of all the channels in the patch membrane that were simultaneously closed. From the two current levels, with all the channels either simultaneously open or closed, we could count the real number of the channels in the patch membrane. Further, to confirm the real number of channels per patch membrane, we calculated the reliability of the estimated number of channels per patch membrane as the real number as previously described (Marunaka and Eaton, 1991; Marunaka and Tohda, 1993). If the probability of the reliability was >0.95, we used the estimated number of the channel per patch membrane for calculation of the P_o of the channel. P_o was calculated using the estimated number of channels per patch as determined by the methods described above.

cAMP Assay

The intracellular cAMP was measured in a similar way described previously (Niisato and Marunaka, 1997*a*, 1997*b*). Before (basal) or after the cells were stimulated with 1 mM IBMX for 3 and 30 min, the medium was aspirated, ice-cold 6% trichloro acetate was added to the cells and incubated on ice for an additional 30 min. After centrifugation at 2,000 *g* for 15 min at 4°C, the supernatants were washed four times with water-saturated diethyl ether. The lower aqueous extracts were lyophilized. For cAMP assay, the samples (dried extracts) were dissolved with the appropriate volume of assay buffer. The concentrations of cAMP in the samples were determined with commercially available cAMP enzyme immunoassay kit (Amersham Corp., Arlington Heights, IL).

Chemicals

All chemicals were purchased from Sigma Chemical Co. (St. Louis, MO) unless otherwise indicated.

Statistical Analyses

Results are presented as mean ± SD. Statistical significance was tested with Student's t test or ANOVA as appropriate. $P < 0.05$ was considered significant.

RESULTS

Single Channel Current Traces in a Cell-attached Patch before and after Application of IBMX

Fig. 1 illustrates representative single-channel current traces from a cell-attached patch formed on the apical membrane at the resting membrane potentials before and after application of 1 mM IBMX. Before application of IBMX, the P_o of the channel was low (Fig. 1 *A*). IBMX stably increased the P_o for up to 30 min after its application (Fig. 1 *B*). The time course of IBMX-induced increase in P_o of the channel is shown in Fig. 2 *A*. The P_o reached a stable value ~3–4 min after application of 1 mM IBMX and remained elevated throughout the time period of our measurement (at least 30 min). The effects of IBMX on P_o increased in a dose-dependent manner (Fig. 2 *B*). IBMX significantly increased intracellular cAMP concentrations from 230 ± 20 fmol/10^5 cells (basal) to 540 ± 40 at 3 min and 1,180 ± 220 fmol/10^5 cells at 30 min after addition of IBMX (1 mM; $n = 4$).

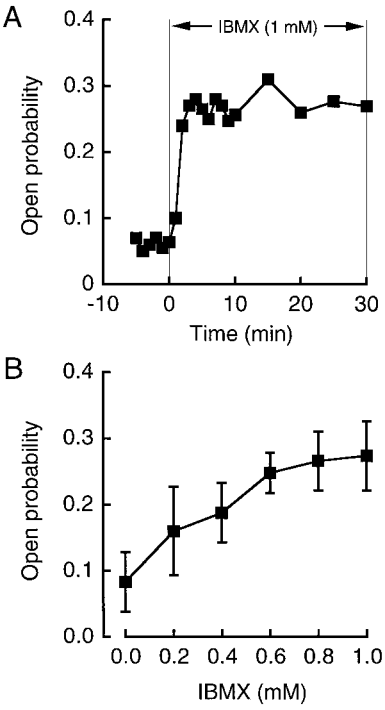

FIGURE 2. The open probability (P_o) of the IBMX (1 mM)-activated channel. (*A*) A typical time course of IBMX-induced change in P_o obtained from a cell-attached patch. Similar time courses could be obtained in three more individual cell-attached patches. (*B*) Effects of IBMX of different concentrations on P_o. The pipette potential was 0 mV. $n = 4$–11.

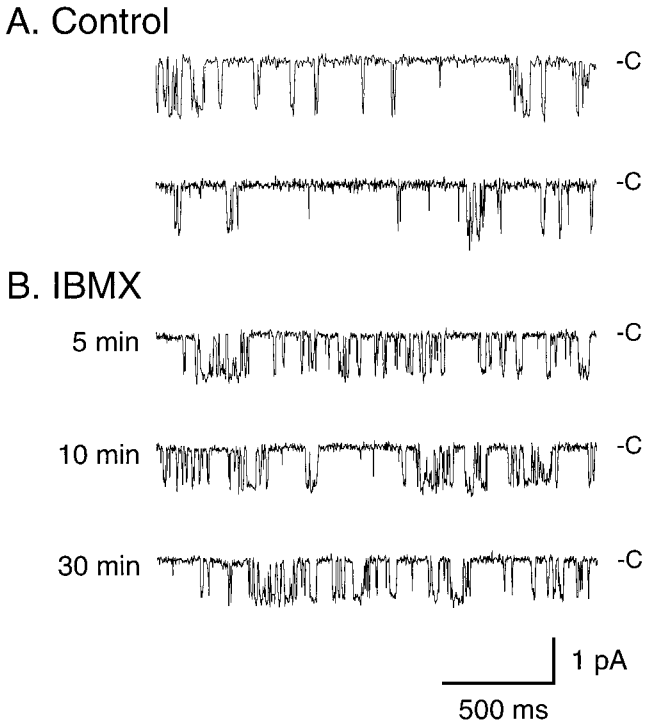

FIGURE 1. Single-channel currents. These currents were obtained from a cell-attached patch formed on the apical membrane with no applied potential (i.e., the resting apical membrane potential) in IBMX-untreated (*A*, *Control*) and -treated (*B*) cells. Closed level of single channel within patch is marked with a horizontal bar and "C" to the right of the trace. Downward deflection indicates inward current across the patch membrane. IBMX (1 mM) increased the P_o of the channel. IBMX (1 mM final concentration) was added to the basolateral solution.

The Current–Voltage Relationship in Cell-attached Patches

The current–voltage (I-V) relationship was nearly linear in cell-attached patches formed on the apical membrane (Fig. 3 *A*). Voltages shown in Fig. 3 *A* indicate the deviation from the resting membrane potential in cell-attached patches. The single-channel conductance was 29.0 ± 0.3 pS ($n = 6$; Fig. 3 *A*, *open circles*). The reversal potential was 45.7 ± 0.7 mV ($n = 6$) more positive than the resting membrane potential. IBMX shifted the I-V relationship to the left by 15 mV (reversal potential = 31.1 ± 1.6 mV; $n = 4$; Fig. 3 *A*) without any effects on single-channel conductance (29.8 ± 0.9 pS, $n = 4$; Fig. 3 *A*, *closed circles*).

Ion Selectivity

This channel had an almost identical permeability to that of Na^+, K^+, Cs^+, and Li^+, but very little permeability to Ca^{2+} or Cl^- compared with that of Na^+ ($P_{Ca}/P_{Na} < 0.005$, $P_{Cl}/P_{Na} < 0.01$; see Fig. 3 *B*). These observations suggest that the IBMX-induced shift in the I-V relationship might be due to a depolarization of the apical membrane.

In general, the sum of Na^+ and K^+ concentrations in the cytosolic and bathing solutions are identical. This means that the reversal potential of an NSC channel (selectivity for Na^+ and K^+, 1:1) is 0 mV. In the absence of IBMX, the reversal potential of the NSC channel in a cell-attached patch formed on the apical membrane was 45.7 mV more positive than the resting potential of the apical membrane (see Fig. 3 *A*, *open circles*). These

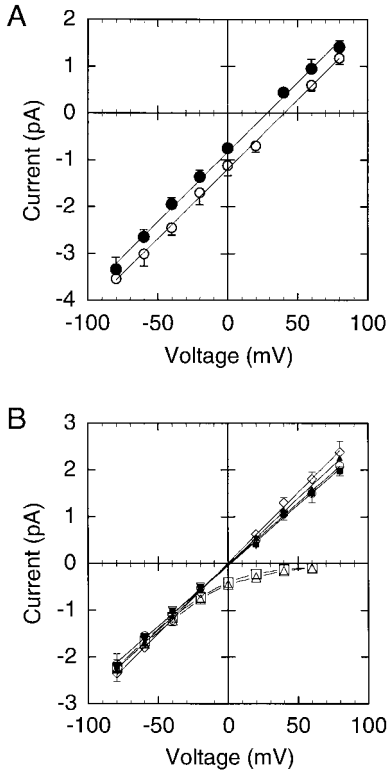

FIGURE 3. (*A*) Current-voltage (I-V) relationship of single channels obtained from cell-attached patches. The I-V relationship was obtained from six (control, *open circles*) and four (IBMX, *closed circles*) individual cell-attached patches. The I-V relationship with IBMX treatment was obtained about 10 min after addition of 1 mM IBMX. $n = 5$. (*B*) Ion selectivity of the IBMX-activated channel. The data were obtained from inside-out patches. The pipette solution contained (mM): 120 NaCl, 1 $CaCl_2$, 1 $MgCl_2$. The bathing (cytosolic) solution contained (mM): 120 NaCl (*open circles*), 120 KCl (*closed squares*), 120 LiCl (*closed triangles*), 120 CsCl (*open diamonds*), 120 K-gluconate (*open inverted triangles*), 120 NMDG-Cl (*open triangles*), or 60 $CaCl_2$ (*open squares*) with 1 $CaCl_2$ and 1 $MgCl_2$. $n = 5$. Voltages are the deviation of the holding potential from the resting membrane potential. The liquid junction potentials were <2 mV. These liquid potentials were not corrected for in the figure. $P_K/P_{Na} \approx P_{Li}/P_{Na} \approx P_{Cs}/P_{Na} \approx 1$, $P_{Cl}/P_{Na} < 0.01$, $P_{Ca}/P_{Na} < 0.005$.

results suggest that the resting potential of the apical membrane without IBMX would be −45.7 mV. Similarly, we can estimate that the apical membrane potential in the presence of 1 mM IBMX would be −31.1 mV.

Effects of IBMX and Stretch on the P_o of the NSC Channels

We explored the relationship between the stretch- and IBMX-induced activation of the NSC channel in more detail. Fig. 4 depicts the effect of stretch on channel activity in the presence and absence of 1 mM IBMX in cell-attached patches. In the case of the IBMX-activated channel, P_o was measured ~10 min after application of 1 mM IBMX. A negative pressure of 60 cm H_2O (stretch) was applied to the pipette. In the absence of IBMX, application of a negative pressure increased the P_o (Fig. 4 *A, a*) proportionately to the magnitude of the negative pressure (Fig. 4 *B, open circles*). IBMX increased P_o in the absence of stretch (Fig. 4 *A, a* and *b*). However, application of a negative pressure of 60 cm H_2O, which had the maximum effect on the P_o of the channel in the absence of IBMX, had no further effect on the IBMX-activated channel (Fig. 4, *A, b* and *B, closed circles*), indicating that the mechanical (stretch) stimulation was not additive to the biochemical (IBMX) stimulation. These observations suggest that the biochemical activation of the NSC channel might induce some tension (or stress) on the membrane analogous to that generated by the mechanical process (stretch).

Single Channel Kinetics

Fig. 5 illustrates open and closed time-interval histograms obtained from cell-attached patches in the absence of applied potential. The open time-interval histogram obtained from an NSC channel without IBMX treatment or application of stretch (control) was fitted by one exponential function (Fig. 5 *A*). The mean open time was 3.9 ms (Table I). In contrast, the closed time-interval histogram without IBMX treatment or application of stretch (control) was fitted by two exponential functions (Fig. 5 *A*). The mean closed times were 2.0 and 32.3 ms (Table I). The open time interval histogram obtained from an NSC channel with IBMX treatment was also fitted by one exponential function (Fig. 5 *B*). The mean open time was 4.2 ms (Table I). Similar to the control experiment, the closed time-interval histogram with IBMX treatment was fitted by two exponential functions (Fig. 5 *B*). The mean closed times were 2.3 and 34.9 ms (Table I). These results indicate that although IBMX increases the P_o, the mean values of open or closed times do not change significantly with application of IBMX. To study how IBMX could increase the P_o without any detectable changes in open and closed times, we compared the frequency of events staying at each state. IBMX increased the frequency of the short closed events and decreased the frequency of the long closed events (Table I) leading to an increase in the P_o of the channel (see models of channel kinetics in DISCUSSION for details). The effects of stretch on the single channel kinetics and other channel properties were the same as those of IBMX (Fig. 5 and Table I).

Effects of Cytochalasin D on the P_o of the Basal, IBMX-, and Stretch-activated NSC Channels

The actin cytoskeleton has been demonstrated to modulate the activity of ion channels (Prat et al., 1993*a*, 1993*b*) and may also participate in sensing mechanical deformation (Sadoshima et al., 1993). As cytochalasin D (CD) is known to depolymerize actin filaments in A6 cells (Verrey et al., 1995), we studied the effects of this cytoskeletal disrupting agent on the channel activity. CD decreased the P_o of the IBMX- or stretch-activated channel to the basal level (Fig. 6) consistent with the concept that disruption of the actin cytoskeleton abrogated the response of the NSC channel to IBMX or stretch. However, CD had no significant effects on the P_o of the basal channel (Fig. 6 *C, Control*). These observations imply that while the IBMX- and stretch-induced

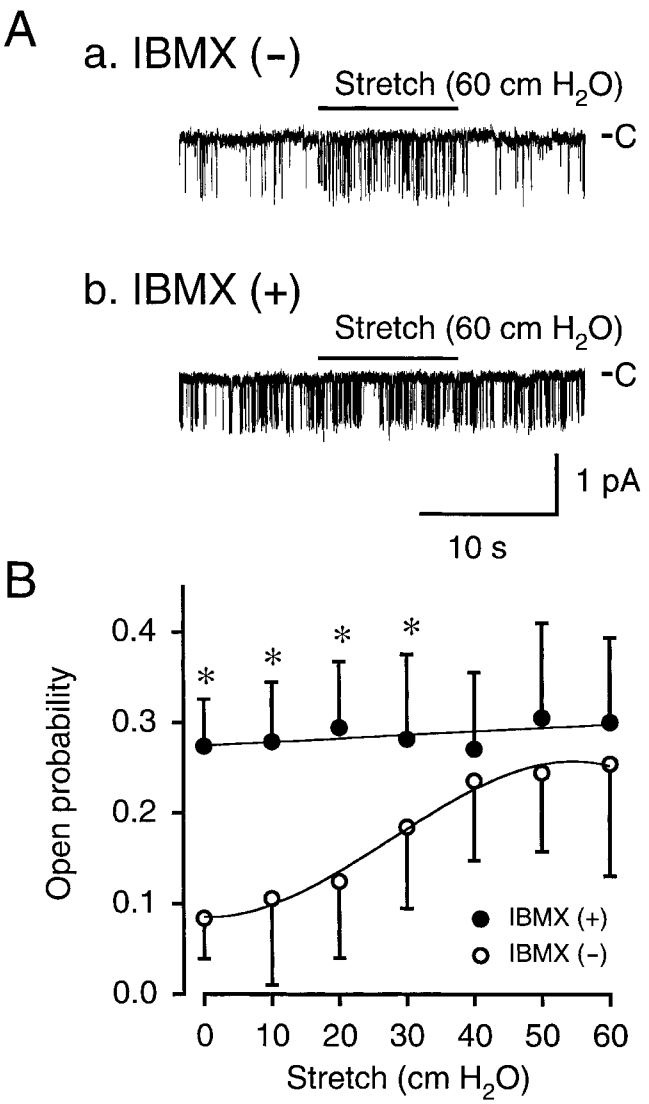

FIGURE 4. Effects of negative pressure (stretch) on the open probability (P_o) of the NSC channel obtained from cell-attached patches formed on the apical membrane at no applied potential (the resting membrane potential) in IBMX-untreated and -treated cells. (*A*) Representative traces of the single channel current with and without a negative pressure of 60 cm H_2O (*Stretch*) in IBMX-untreated (*a*) and -treated (*b*) cells. In the untreated IBMX cell (*a*), the channel stayed longer in an open state during the period indicated by horizontal bar above the trace when the stretch (60 cm H_2O) was applied than without. In contrast, the stretch-induced activation was not observed in the IBMX-treated cell (*b*). (*B*) The statistical results of the P_o against the stretch of various strength in the IBMX-untreated (*IBMX* (–), *open circles*) and -treated (*IBMX* (+), *closed circles*) cells are shown. The P_o of the NSC channel shown here was measured at no applied potential (i.e., the resting membrane potential) from the single-channel recording for ~2 min. The results of IBMX treatment shown here were obtained ~10 min after addition of IBMX (the final concentration = 1 mM) to the basolateral solution. IBMX significantly increased the P_o of the channel without application of the stretch and with application of a relatively low strength of stretch (*≤30 cm H_2O). In the IBMX-untreated cells, the P_o of the NSC channel with application of the stretch was significantly larger than that with no application of the stretch (*IBMX* (–), *open circles*). However, no significant effects of stretch were observed in the IBMX-treated cells (*IBMX* (+), *closed circles*). $n = 11$.

activation of the NSC channel was dependent on an intact actin cytoskeleton, the basal channel activity (P_o) was not.

Effects of H89 on the P_o of the Basal, IBMX-, and Stretch-activated NSC Channels

Pretreatment of cells with H89 (0.5 μM, 2 h), an inhibitor of cAMP-dependent protein kinase A, significantly decreased the P_o of the NSC channel (Fig. 7, *A* and *B*, *Control*), and abolished the response of the channel to IBMX or stretch (Fig. 7, *A* and *B*, *IBMX* and *Stretch*). These observations indicate that all basal activity, and IBMX- and stretch-induced activation of the NSC channel, may be mediated by PKA-dependent phosphorylation, either of the channel itself or of associated regulatory proteins.

DISCUSSION

We have previously reported the presence of a stretch-activated NSC channel that is also transiently activated by AVT (Marunaka et al., 1994). However, the relationship between the AVT- and stretch-induced activation of this channel was incompletely understood. Since the AVT-induced activation was found to be transient, we were unable to characterize this relationship in detail. In the present study, we found that IBMX stably activated the NSC channel, thus enabling us to develop a model system in which we could investigate the relationship between the cAMP (a second messenger of AVT)-induced and mechanical (stretch) activation of the NSC channel.

The activity of the stretch-activated channels is known to be dependent, at least in part, on actin filaments (Mills et al., 1994). However, the link between cAMP-dependent activation, stretch-induced activation, and the cytoskeleton was unclear. Recently, Prat et al. (1993*a*, 1993*b*) have reported that the catalytic subunit of PKA activates a 9-pS Na^+-selective channel ($P_{Na}/P_K \approx 4$) in A6 cells cultured on impermeable supports (glass cover slips), and that activation of the channel by PKA requires actin filaments. However, no information about the action of stretch on the 9-pS Na^+-selective channel was available (indeed, this channel may not be activated by stretch). Therefore, although the actin filaments are purportedly required for PKA catalytic subunit-induced activation of the channel, the relationship between activation by PKA, stretch, and the cytoskeleton was unclear. In the present study, we have demonstrated that the mechanism of stretch-induced activation is very similar to that of cAMP-induced (PKA-mediated) activation of

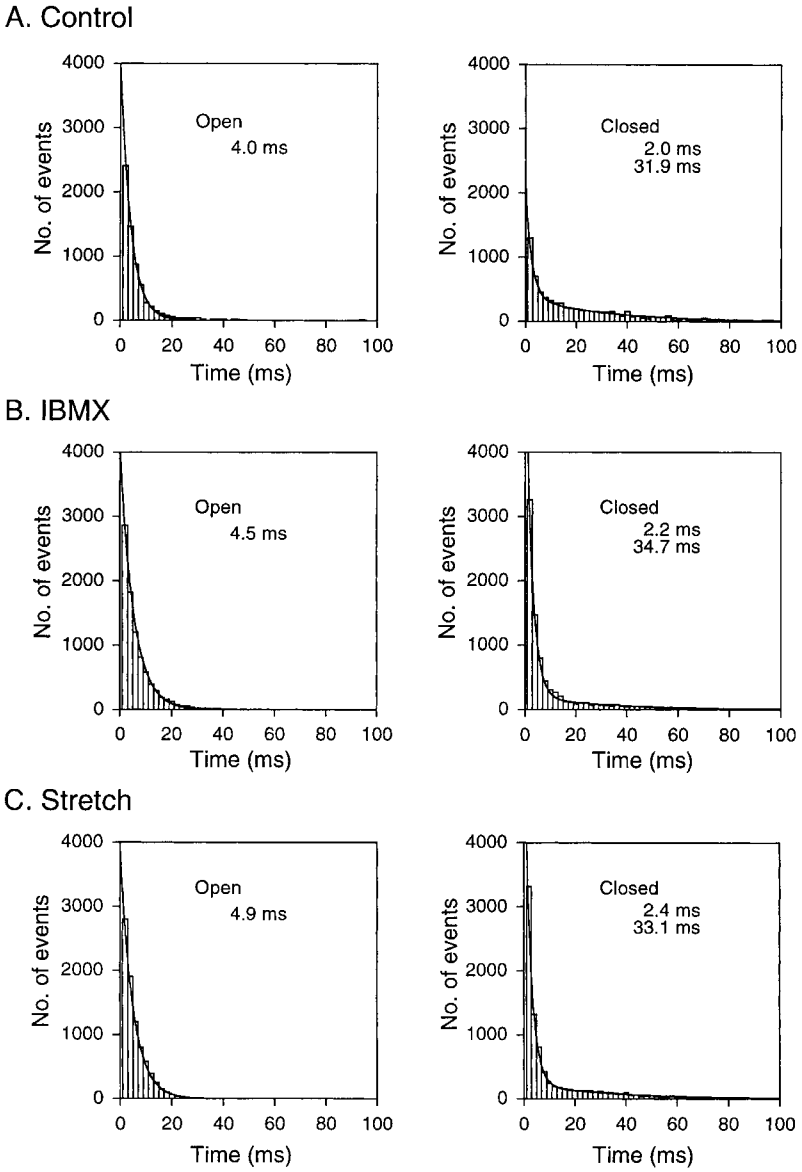

FIGURE 5. Open and closed time-interval histograms. Open and closed time-interval histograms obtained from a cell-attached patch at no applied potential (the resting membrane potential) without any treatment (*A, Control*), with 1 mM IBMX treatment (*B, IBMX*), or with application of stretch (*C, Stretch*; a negative pressure of 60 cm H_2O) are shown. Bars show the number of single channel events during the indicated time periods when the channel stayed in the open or closed state. Open- and closed-interval histograms are respectively fitted by one and two exponential functions (*solid lines*). Mean open times are 4.0 ms in the control, 4.5 ms in the IBMX-activated channel, and 4.9 ms in the stretch-activated channel. Mean closed times are 2.0 and 31.9 ms in the control, 2.2 and 34.7 ms in the IBMX-activated, and 2.4 and 33.1 ms in the stretch-activated channel. The open and closed time-interval histograms in an IBMX-activated channel was obtained about 10 min after addition of 1 mM IBMX to the basolateral solution.

the channel and that both are contingent on intact actin microfilaments. Moreover, the basal activity of the NSC channel was found to be dependent on PKA-mediated phosphorylation but apparently independent of actin filaments.

In the present study, we suggest that the cAMP-activated NSC channel has the same characteristics in single channel kinetics and sensitivity to cytochalasin D as the stretch-activated NSC channel, and their stimulation depends upon phosphorylation and actin filaments. Possible explanations for these results include: (*a*) that phosphorylation of the actin filaments (Prat et al., 1993*b*) produces cortical tension similar to that caused by stretch, and this tension activates the NSC channel, or (*b*) that stretch stimulates the phosphorylation of actin filaments, which in turn activate the NSC channel. To test the latter possibility, we endeavored to determine whether the stretch of the patch membrane induced the phosphorylation of actin filaments. However, given the limitations of our current system, we were not able to detect phosphorylation of actin filaments induced by this force, likely because the magnitude of stretch by the patch pipette was too small or localized to allow detection of phosphorylation of small numbers of actin filaments. Thus, it remains to be determined whether stretch stimulates phosphorylation of actin filaments. Further, one would need to develop methods suitable for the measurement of membrane tension that are sensitive enough to allow detection of the effects of cAMP and stretch in order to test the former possibility and reach firm conclusions.

We have previously reported that depolarization in-

TABLE I

The Mean Open and Closed Times, the Number of Events in Each State, and the Fractional Time of Each State of the Basal (Control), IBMX-, and Stretch-activated NSC Channels

		Closed	
	Open	Short	Long
Mean times (ms)			
Control	3.9 ± 1.1	2.0 ± 0.7	32.3 ± 10.0
IBMX	4.2 ± 2.0	2.3 ± 1.5	34.9 ± 13.0
Stretch	4.8 ± 2.0	2.4 ± 1.6	31.5 ± 15.1
Fractional number of events (%)			
Control	49.8 ± 3.2	11.2 ± 0.5	39.0 ± 0.6
IBMX	49.9 ± 0.4	32.6 ± 0.3*	17.6 ± 0.3*
Stretch	49.6 ± 0.4	32.9 ± 0.3*	17.5 ± 0.2*
Fractional time (%)			
Control	13.8 ± 4.9	1.6 ± 0.6	84.6 ± 5.7
IBMX	24.4 ± 10.9‡	7.6 ± 3.1*	68.0 ± 8.5*
Stretch	27.3 ± 6.3*	8.4 ± 4.8§	64.3 ± 10.2*

These events were collected from ~3-min records obtained from control (without IBMX treatment of application of stretch), IBMX-, and stretch-activated channels in cell-attached patches. The parameters in the IBMX-activated channel were not significantly different from those in the stretch-activated channel. *$P < 0.001$; ‡$P < 0.05$; §$P < 0.005$. $n = 7$.

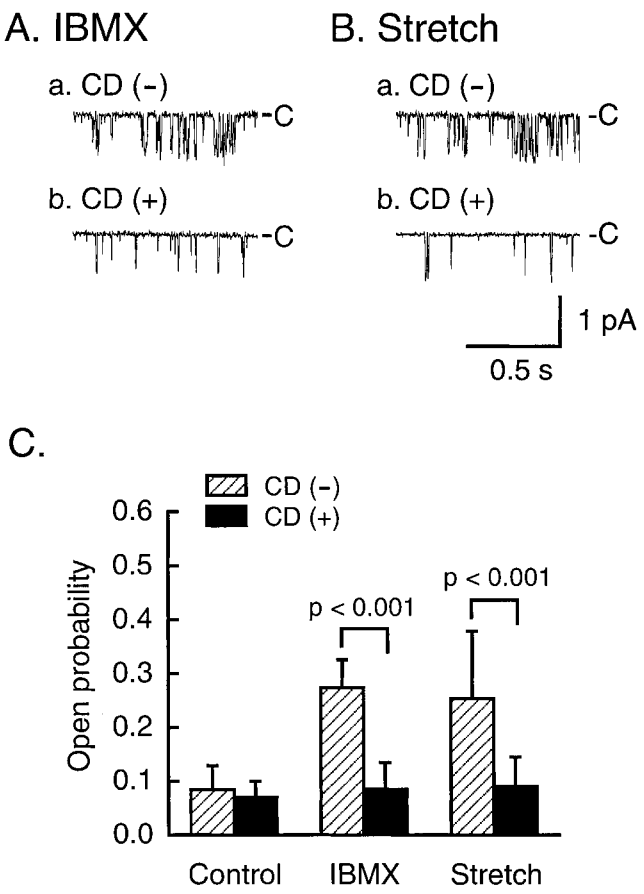

FIGURE 6. Effects of cytochalasin D (*CD*) on the P_o of the NSC channel obtained in cell-attached patches formed on the apical membrane at no applied potential (the resting membrane potential) in the basal, IBMX-, and stretch-(a negative pressure of 60 cm H_2O) activated channels. (*A*) Representative traces of the single channel currents obtained from the IBMX-activated channel with and without CD (5 μM) treatment. (*B*) Representative traces of the single channel current obtained from the stretch-activated channel with and without CD (5 μM) treatment. (*C*) The statistical result of the effects of CD on the P_o of the basal, IBMX-, and stretch-activated channel. The P_o of the NSC channels shown here was measured at no applied potential (i.e., the resting membrane potential) from a single channel recording for ~2 min. In the IBMX- (1 mM, 10 min) and stretch-activated channels, the P_o of the NSC channel was decreased by the treatment with CD; however, CD had no significant effects on the P_o of the basal NSC channel. Further, the P_o of the channel with IBMX or stretch in the presence of CD was not significantly different from that of the basal (control) channel. The results shown here with CD treatment were obtained about 10 min after addition of 5 μM CD to the apical membrane. n = ~11–16.

creases the P_o of the NSC channel (Marunaka et al., 1994). One interpretation of this observation is that the IBMX-induced increase in the P_o of the NSC channel is consequent to depolarization of the apical membrane, since IBMX induced a shift of the I-V relationship by 15 mV to the left without affecting the ion selectivity. Accordingly, we studied the voltage dependency of the IBMX-stimulated NSC channel and found that the IBMX-stimulated NSC channel did not show any voltage dependency within the range of ±40 mV in cell-attached patches; i.e., $P_o = 0.26 \pm 0.04$ at −40 mV, 0.25 ± 0.04 at −20 mV, 0.28 ± 0.05 at 0 mV, 0.26 ± 0.04 at 20 mV, and 0.29± 0.03 at 40 mV (voltages indicate the deviation from the resting membrane potential in cell-attached patches; $n = 4$). We interpret these data to mean that the IBMX-induced increase in the P_o of the NSC channel was not due to the depolarization of the apical membrane but rather due to phosphorylation of the channel and/or channel-associated proteins including actin filaments.

In the present study, we demonstrated that either IBMX or stretch increases the P_o of the NSC channel without changing the mean open or closed time. As an explanation for these observations, we considered three types of linear models of channel gating kinetics designated I, II, and III, since three possible kinetic schemes as linear models of channel gating kinetics are compatible with the observation that the channel has one open and two closed states, irrespective of application of IBMX or stretch. In the ensuing discussion, each model will be discussed separately.

Model I. Eq. A shows a model of the kinetics of the NSC channel.

$$C_S \underset{k_{-1}}{\overset{k_1}{\rightleftharpoons}} O \underset{k_{-2}}{\overset{k_2}{\rightleftharpoons}} C_L, \qquad \text{(A)}$$

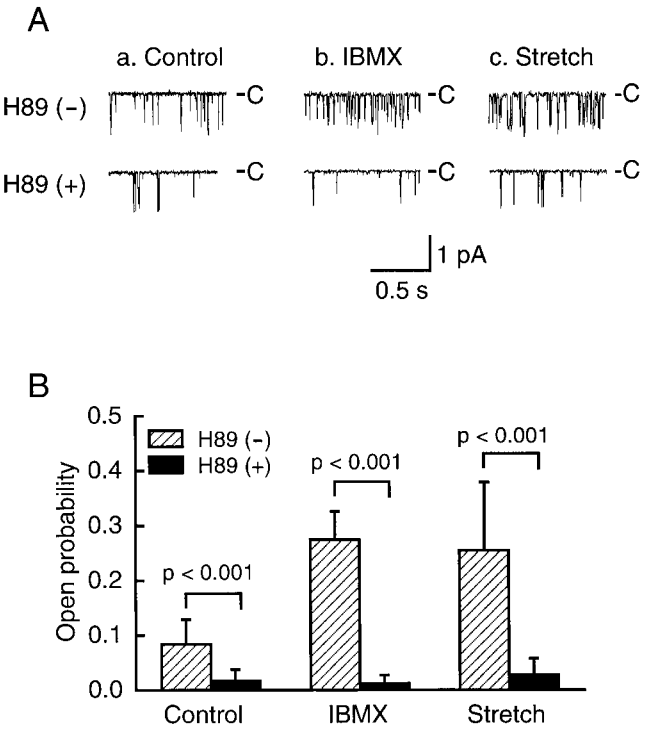

FIGURE 7. Effects of H89 on the P_o of the basal, IBMX-, and stretch-activated NSC channels obtained in cell-attached patches formed on the apical membrane at no applied potential (the resting membrane potential). (*A*) Representative traces of the single channel currents obtained from the basal (*a, Control*), IBMX-activated (*b, IBMX*), and stretch-activated (*c, Stretch*) channels with and without H89 pretreatment (0.5 μM, 2 h). H89 decreased the P_o of the channel in each case. (*B*) The statistical result of the effects of H89 on the P_o of the basal (*Control*), IBMX-activated (*IBMX*), and stretch-activated (*Stretch*) channels. In all the basal, IBMX-, and stretch-activated NSC channels, the P_o of the NSC channel was significantly decreased by the treatment of H89. $n = 11$.

where O is the open state; C_S, the short closed state; C_L, the long closed state; k, the leaving rate from each state. Initially, we estimated each rate under the basal (control) condition. Since the mean value of the short closed time was 2.0 ms, k_1 was 500 s^{-1}; since the mean value of the long closed time was 32.3 ms, k_{-2} was 31 s^{-1}. The relationship between the mean open time (τ_O), k_2, and k_1 is as follows:

$$\tau_O = \frac{1}{k_{-1} + k_2}. \quad \text{(B)}$$

Further, the event numbers of the channel staying in the short (N_{C_S}) and long (N_{C_L}) closed states depend upon k_{-1} and k_2, respectively (see Eq. A). Namely, N_{C_L} and N_{C_S} are respectively expressed as follows:

$$N_{C_L} = \frac{k_2}{k_{-1} + k_2} N_O, \quad \text{(C)}$$

$$N_{C_S} = \frac{k_{-1}}{k_{-1} + k_2} N_O, \quad \text{(D)}$$

where N_O is the event number of the channel staying in the open state. From these Eqs. C and D, the following equation is derived.

$$\frac{N_{C_L}}{N_{C_S}} = \frac{k_2}{k_{-1}}. \quad \text{(E)}$$

From the Eqs. B and E, k_{-1} and k_2 were estimated (Table II). Similar to the control condition, the kinetics of the IBMX-activated NSC channel were estimated (Table II). As shown in Table II, IBMX increases the P_o by decreasing k_2 (the leaving rate for the long closed state from the open state) and increasing k_{-1} (the leaving rate for the short closed state from the open state) with little effect on k_1 or k_{-2} (the leaving rate from each closed state). In other words, without affecting the closed states, IBMX treatment favors the channel leaving the open state for the short closed state as compared with the long closed state. Further, as a result of a decrease in the leaving rate for the long closed state and an increase in the leaving rate for the short closed state, IBMX (presumably via PKA-mediated phosphorylation) did not change the mean open time. According to this model, phosphorylation would affect the channel only when it remained in the open state. In the case of the stretch-induced activation of the channel, the same phenomenon would occur as with IBMX-induced activation.

Model II. Eq. F illustrates a model of the kinetics of the NSC channel.

$$C_L \underset{k_{-3}}{\overset{k_3}{\rightleftharpoons}} C_s \underset{k_{-4}}{\overset{k_4}{\rightleftharpoons}} O, \quad \text{(F)}$$

where O is the open state, C_S is the short closed state, C_L is the long closed state, k is the leaving rate from each state. In the initial analysis, each rate was estimated under the basal (control) condition. Since the mean value of the short closed time was 2.0 ms, k_{-4} was 500 s^{-1}; since the mean value of the open time was 4.0 ms, k_{-4} was 250 s^{-1}. The mean long closed time (τ_{CL}) is expressed as follows:

$$\tau_{C_L} = \frac{1}{k_{-3}} + \frac{1}{k_3} + \frac{1}{k_4}. \quad \text{(G)}$$

TABLE II

The Rates Leaving from Each State in the Basal (Control), IBMX-, and Stretch-activated NSC Channels in Model I

	Rate (s^{-1})			
	k_1	k_2	k_{-1}	k_{-2}
Control	590 ± 310	220 ± 60	60 ± 20	30 ± 10
IBMX	660 ± 470	100 ± 50*	200 ± 100*	30 ± 10
Stretch	820 ± 170	90 ± 50*	170 ± 100‡	40 ± 10

There were no significant differences between the rates of the IBMX- and stretch-activated NSC channels. *$P < 0.005$; ‡$P < 0.025$. $n = 7$.

Further, the event numbers of the channel staying in the short (N_{C_S}) and long (N_{C_L}) closed states depend upon k_4 and k_{-3}, respectively. In other words, the relationship between N_{C_L} and N_{C_S} can be expressed as follows:

$$\frac{N_{C_S}}{N_{C_L}} = \frac{k_4}{k_{-3}}. \quad \text{(H)}$$

From the Eqs. G and H, k_3 and k_{-3} were estimated (Table III). In an analogous manner, the kinetics of the IBMX-activated NSC channel was estimated (Table III). As shown in Table III, IBMX increases the P_o by only decreasing k_{-3} (the leaving rate for the long closed state from the short closed state) without any changes in other rates. In other words, without affecting the open or long closed state, IBMX decreases the chance for the channel to leave the short closed state for the long closed state. Although IBMX decreased the leaving rate for the long closed state from the short closed state, we could not detect any significant changes in the mean long closed time induced by IBMX (via PKA-dependent phosphorylation). Since k_{-3} and k_4 are much larger than k_3 (Table III), the mean long closed time is dependent mainly upon the leaving rate from the long closed state for the short closed state (k_3; see Eqs. F and G). The IBMX-induced change in k_{-3} (the leaving rate for the long closed state from the short closed state) would be too small to be detected as a change in the mean long closed time, accounting for the lack of significant change observed in our study. In this model, we suggest that phosphorylation affects the channel only when it remains in the short closed state. In the case of the stretch-induced activation of the channel, the same phenomenon occurred as with IBMX-induced activation.

Model III. A third model was considered as follows:

$$C_S \underset{k_{-5}}{\overset{k_5}{\rightleftharpoons}} C_L \underset{k_{-6}}{\overset{k_6}{\rightleftharpoons}} O, \quad \text{(I)}$$

In the case of Model III, each rate was estimated as described for Model II. Specifically, in control, k_5, k_{-5}, and k_6 were estimated to be 40 ± 10 s^{-1}, 2,090 ± 1,060 s^{-1}, and 590 ± 310 s^{-1}, respectively. The residency time of the channel in "C_S" ($1/k_5$) is much longer than that in "C_L" ($1/(k_{-5} + k_6)$). This is inconsistent with the definition of C_S and C_L. Accordingly, we can eliminate Model III as a valid explanation for our observations.

Further, a nonlinear model merits consideration as follows:

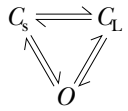

Unfortunately, in the absence of an experimental method for determining individual rates from one state to another (i.e., specific blocker for communication between each state), such a nonlinear model cannot be evaluated.

Among three linear models, we consider Model II to be the most suitable for the following reasons. As discussed above, Model III can be excluded. If Model I is chosen, the rate of entering the long closed state should decrease just enough to compensate for an increase in the rate of entering the short closed state when IBMX or stretch activates the channel. It is difficult to envision a physical coupling mechanism of the channel that is able to compensate exactly for the changes in gating kinetics of the other. On the other hand, in Model II, if IBMX or stretch decreases the chance of the channel leaving the short closed state for the long closed state, it is sufficient to explain the observations outlined in the current study. For these reasons, we suggest that Model II is the most suitable one.

Unlike the NSC channel studied here, most NSC channels have some permeability for Ca^{2+} in addition to Na^+ and K^+ (Hoyer et al., 1994; Sackin, 1995), including another NSC channel in A6 cells (Kawahara and Matsuzaki, 1993). In general, the NSC channel that responds to stretch contributes to an increase in the cytosolic Ca^{2+} concentration. The NSC channel reported here, however, does not contribute to a change in the cytosolic Ca^{2+} concentration, but only to Na^+ and K^+ transport.

In conclusion, we have demonstrated that: (*a*) IBMX stably activates a 29-pS NSC channel, unlike vasotocin (an antidiuretic hormone); (*b*) the basal NSC channel responds to stretch while the IBMX-activated channel does not; (*c*) IBMX-induced activation is very similar to the stretch-induced activation; (*d*) IBMX- and stretch-induced activation of the channel requires polymerized actin filaments, which appear to make no contribution to the basal channel activity; (*e*) phosphorylation maintains the basal, IBMX-, and stretch-activated channel activity; (*f*) a linear gating kinetic model "$C_L \leftrightarrow C_S \leftrightarrow O$" is the most suitable of the three possible linear models; (*g*) according to Model "$C_L \leftrightarrow C_S \leftrightarrow O$," only the leaving rate of the channel for C_L from C_S is decreased by application of IBMX or stretch, resulting in an increase in the P_o of the channel.

TABLE III

The Rates Leaving from Each State in the Basal (Control), IBMX-, and Stretch-activated NSC Channels in Model II

	Rate (s^{-1})			
	k_3	k_4	k_{-3}	k_{-4}
Control	40 ± 10	590 ± 310	2090 ± 1060	280 ± 80
IBMX	40 ± 10	660 ± 470	350 ± 230*	300 ± 150
Stretch	50 ± 20	820 ± 170	440 ± 80*	260 ± 150

There were no significant differences between the rates of the IBMX- and stretch-activated NSC channels. *$P < 0.005$. $n = 7$.

The authors thank Dr. C.E. Bear for critically reading the manuscript.

This work was supported by a Grant-in-Aid from the Kidney Foundation of Canada to Y. Marunaka, and partly supported by Grants-in-Aid from the Medical Research Council of Canada to G.P. Downey and Y. Marunaka (Group Grants and MA13494), the Ontario Thoracic Society (Block Term Grant), and MPG Research Fund to Y. Marunaka. Dr. Marunaka is a Scholar of the Medical Research Council of Canada. Dr. Downey is a Clinician Scientist of the Ontario Ministry of Health.

Original version received 29 November 1996 and accepted version received 10 July 1997.

REFERENCES

Benos, D.J., G. Saccomani, B.M. Brenner, and S. Sariban-Sohraby. 1986. Purification and characterization of the amiloride-sensitive sodium channel from A6 cultured cells and bovine renal papilla. *Proc. Natl. Acad. Sci. USA.* 83:8525–8529.

Chalfant, M.L., B. Coupaye-Gerard, and T.R. Kleyman. 1993. Distinct regulation of Na^+ reabsorption and Cl^- secretion by arginine vasopressin in the amphibian cell line A6. *Am. J. Physiol.* 264: C1480–C1488.

Doi, Y., and Y. Marunaka. 1995. Amiloride-sensitive and HCO_3^--dependent ion transport activated by aldosterone and vasotocin in A6 cells. *Am. J. Physiol.* 268:C762–C770.

Garty, H., and D.J. Benos. 1988. Characteristics and regulatory mechanisms of the amiloride- blockable Na^+ channel. *Physiol. Rev.* 68:309–373.

Hoyer, J., A. Distler, W. Haase, and H. Gogelein. 1994. Ca^{2+} influx through stretch-activated cation channels activates maxi K^+ channels in porcine endocardial endothelium. *Proc. Natl. Acad. Sci. USA.* 91:2367–2371.

Kawahara, K., and K. Matsuzaki. 1993. A stretch-activated cation channel in the apical membrane of A6 cells. *Jpn. J. Physiol.* 43: 817–832.

Marunaka, Y. 1993. Modification of Ca^{2+}-sensitivity of Ca^{2+}-activated Cl^- channel by vasopressin and cholera toxin. *Jpn. J. Physiol.* 43:553–560.

Marunaka, Y. 1996*a*. Physiological requirement of aldosterone action on Na^+/K^+ pump in ADH-stimulated Na^+ absorption in renal epithelium. *Jpn. J. Physiol.* 46: 357–361.

Marunaka, Y. 1996*b*. Amiloride-blockable Ca^{2+}-activated Na^+-permeant channels in the fetal distal lung epithelium. *Pflugers Arch.* 431:748–756.

Marunaka, Y., and D.C. Eaton. 1990*a*. Chloride channels in the apical membrane of a distal nephron A6 cell line. *Am. J. Physiol.* 258: C352–C368.

Marunaka, Y., and D.C. Eaton. 1990*b*. Effects of insulin and phosphatase on a Ca^{2+}-dependent Cl^- channel in a distal nephron cell line (A6). *J. Gen. Physiol.* 95:773–789.

Marunaka, Y., and D.C. Eaton. 1991. Effects of vasopressin and cAMP on single amiloride-blockable Na channels. *Am. J. Physiol.* 260:C1071–C1084.

Marunaka, Y., N. Hagiwara, and H. Tohda. 1992. Insulin activates single amiloride-blockable Na channels in a distal nephron cell line (A6). *Am. J. Physiol.* 263:F392–F400.

Marunaka, Y., and H. Tohda. 1993. Effects of vasopressin on single Cl^- channels in the apical membrane of distal nephron epithelium (A6). *Biochim. Biophys. Acta.* 1153:105–110.

Marunaka, Y., H. Tohda, N. Hagiwara, and T. Nakahari. 1994. Antidiuretic hormone-responding non-selective cation channel in distal nephron epithelium (A6). *Am. J. Physiol.* 266:C1513–C1522.

Mills, J.W., E.M. Schwiebert, and B.A. Stanton. 1994. The cytoskeleton and membrane transport. *Curr. Opin. Nephrol. Hypertens.* 3: 529–534.

Nakahari, T., and Y. Marunaka. 1995. ADH-evoked $[Cl^-]_i$-dependent transient in whole cell current of distal nephron cell line A6. *Am. J. Physiol.* 268:F64–F72.

Nakahari, T., and Y. Marunaka. 1996. ADH action on whole-cell currents by cytosolic Ca^{2+}-dependent pathways in aldosterone-treated A6 cells. *J. Membr. Biol.* 154:35–44.

Niisato, N., and Y. Marunaka. 1997*a*. Cross talk of bumetanide-sensitive and HCO_3^--dependent transporters activated by IBMX in renal epithelial A6 cells. *J. Membr. Biol.* 157:53–61.

Niisato, N., and Y. Marunaka. 1997*b*. Regulation of Cl^- transport by IBMX in renal A6 epithelium. *Pflugers Arch.* 434:227–233.

Niisato, N., and Y. Marunaka. 1997*c*. Hyposmolality-induced enhancement of ADH action on amiloride-sensitive Isc in renal epithelial A6 cells. *Jpn. J. Physiol.* 47:131–137.

Palmer, L.G. 1992. Epithelial Na channels: function and diversity. *Annu. Rev. Physiol.* 54:51–66.

Perkins, F.M., and J.S. Handler. 1981. Transport properties of toad kidney epithelia in culture. *Am. J. Physiol.* 241:C154–C159.

Prat, A.G., D.A. Ausiello, and H.F. Cantiello. 1993*a*. Vasopressin and protein kinase A activate G protein-sensitive epithelial Na^+ channels. *Am. J. Physiol.* 265:C218–C223.

Prat, A.G., A.M. Bertorello, D.A. Ausiello, and H.F. Cantiello. 1993*b*. Activation of epithelial Na^+ channels by protein kinase A requires actin filaments. *Am. J. Physiol.* 265:C224–C333.

Sackin, H. 1995. Mechanosensitive channels. *Annu. Rev. Physiol.* 57: 333–353.

Sadoshima, J., Y. Xu, H.S. Slayter, and S. Izumo. 1993. Autocrine release of angiotensin II mediates stretch-induced hypertrophy of cardiac myocytes in vitro. *Cell.* 75:977–984.

Sariban-Sohraby, S., E.J. Sorscher, B.M. Brenner, and D.J. Benos. 1988. Phosphorylation of a single subunit of the epithelial Na^+ channel protein following vasopressin treatment of A6 cells. *J. Biol. Chem.* 263:13875–13879.

Smith, P.R., and D.J. Benos. 1991. Epithelial Na^+ channels. *Annu. Rev. Physiol.* 53:509–530.

Verrey, F., P. Groscurth, and U. Bolliger. 1995. Cytoskeletal disruption in A6 kidney cells: impact on endo/exocytosis and NaCl transport regulation by antidiuretic hormone. *J. Membr. Biol.* 145: 193–204.